Cement & Concrete Composites 31 (2009) 731–743

Contents lists available at ScienceDirect

Cement & Concrete Composites

journal homepage: www.elsevier.com/locate/cemconcomp

The behavior of self-compacting concrete containing micro-encapsulated Phase Change Materials

M. Hunger [a,*], A.G. Entrop [a], I. Mandilaras [b], H.J.H. Brouwers [a], M. Founti [b]

[a] Department of Construction Management and Engineering, Faculty of Engineering Technology, University of Twente, P.O. Box 217, 7500 AE, Enschede, The Netherlands
[b] Laboratory of Heterogeneous Mixtures and Combustion Systems, School of Mechanical Engineering, National Technical University of Athens, 9, Heroon Polytechniou, Polytechnioupoli Zografou, Athens 15780, Greece

ARTICLE INFO

Article history:
Received 19 November 2008
Received in revised form 10 August 2009
Accepted 11 August 2009
Available online 15 August 2009

Keywords:
PCM
Self-compacting concrete
Latent heat capacity
Hydration heat

ABSTRACT

In order to come to a sustainable built environment the construction industry requires new energy saving concepts. One concept is to use Phase Change Materials (PCM), which have the ability to absorb and to release thermal energy at a specific temperature. This paper presents a set of experiments using different amounts of PCM in self-compacting concrete mixes. The study focuses on the direct mixing of micro-encapsulated PCM with concrete and its influence on the material properties. Therefore, the fresh concrete properties and the hardened properties are investigated. The hardened properties comprise strength tests and a thorough assessment of the thermal properties. It will be shown that increasing PCM amounts lead to lower thermal conductivity and increased heat capacity, which both significantly improve the thermal performance of concrete and therefore save energy. On the other hand a significant loss in strength and micro-structural analysis both indicate that a large part of the capsules is destroyed during the mixing process and releases its paraffin wax filling into the surrounding matrix. However, the compressive strength of our specimens still satisfies the demands of most structural applications.

1. Introduction

Concrete incorporating Phase Change Materials (PCM) can be used to store thermal energy lowering the energy consumption of buildings and increasing thermal comfort [1–3]. Phase Change Materials have the ability to absorb and to release energy in heat form at a specific temperature when their state changes [4]. The heat capacity and high density of concrete combined with the use of the latent heat storage of PCM can provide new energy saving concepts, for example in combination with solar energy. In fresh concrete mixes PCM could be added to prevent high hydration temperature peaks, which can result in higher compressive strength and better durability.

The use of PCM in building materials and components has been researched for multiple years and different materials and components have been regarded to incorporate them (e.g. [3,5–9]). In their research these scholars used furthermore different types of PCM. Sharma et al. [10] distinguish three main groups of PCM: organic, inorganic, and eutectic. Within the group of organic PCM there are two different types: paraffin and non-paraffin compounds. Because the direct use of a micro-encapsulated mixture of paraffins in fresh concrete has not received much attention yet, a mixture of paraffins will be used in this research. It concerns a commercially available product for the building industry with a melting point of 23 °C named Micronal DS 5008 X. According to the product descriptions, it is described as a mixture of paraffin waxes in powder form, encapsulated in polymethyl methacrylate micro-capsules. The technique of micro-encapsulation is used here in order to surround the liquid/solid paraffin phase with a hard shell. This way the liquid paraffin (<23 °C) is transformed into a powder and prevented from entering the surrounding matrix. Due to the encapsulation, it should be theoretically possible to disperse the paraffin in the fresh concrete mix and to melt it without any interaction between the PCM and the concrete constituents.

This research aims to contribute to existing knowledge on the use of micro-encapsulated PCM in self-compacting concrete (SCC) by conducting experiments regarding its behavior during mixing, hydration and after hardening. The properties of three recipes containing 1% PCM, 3% PCM and 5% PCM (by mass of concrete) were compared with one reference mix. Marble powder, a mineral waste material with a particle size distribution similar to the used PCM, has been used to account for the varying PCM amounts. This way all four mixes have a similar grading. The PCM additions correspond to 2.5–12.4% of volume in the mix. The properties of fresh SCC were evaluated using the J-ring test and V-funnel test. During hydration the influence of PCM on the heat development was firstly modeled and secondly monitored in situ. Finally, the hardened concrete was subjected to compressive strength tests and tests to measure its thermal properties. Furthermore, densities

* Corresponding author. Tel.: +31 53 489 6863; fax: +31 53 489 2511.
E-mail address: martinhunger@gmx.at (M. Hunger).

0958-9465/$ - see front matter © 2009 Elsevier Ltd. All rights reserved.
doi:10.1016/j.cemconcomp.2009.08.002

were measured and visual observations were reported. Moreover, the micro-structure has been analyzed by using SEM. In our conclusions we will reveal how the mix design functioned, what the thermal properties of self-compacting concrete containing micro-encapsulated PCM are, and how the loss of compressive strength can be explained.

2. Choice of components – mix design

A practical aim of this research is to prevent high hydration temperature peaks during the first day of hydration. A deliberately high cement dosage of 450 kg/m^3 was selected to come to a significant heat development. Nevertheless, this dosage still represents realistic cement loads, which are in construction practice sometimes notably exceeded. Furthermore, the choice of the binder type can clearly influence the hydration heat development [11]. For this reason a mixture of cement with high fineness (micro-cement) as well as a R type cement with higher clinker content was selected. In detail this mixture is composed of one part Ultrafin 12 and two parts of a CEM I 32.5 R. Ultrafin 12 is a micro-cement of the type CEM I 52.5 R.

In order to account for the varying PCM amounts in the mixes, a non reactive material with comparable particle size distribution is necessary to substitute the respective PCM volume. This way it is assured that all mixes are comparable from the granulometric point of view. Accordingly, all respective variations compared to the (PCM-free) reference mix can be assigned to the influence of the PCM. For this test a dolomitic marble powder is selected, which in former research was successfully applied in SCC production [12]. PCM and marble powder were substituted on volumetric base and are of similar particle size distribution regarding the powders of our disposal. The 5% mix is an exception since the PCM volume in this case is higher than the available marble volume. Therefore, a slightly higher fines content is present in this mix. The particle size distributions of all applied powder types are given in Fig. 1.

Moreover, the concrete is designed with common aggregates like a fine sand 0–1, another 0–4 sand fraction, an intermediate gravel fraction 2–8 and a gravel fraction 4–16. All sand and gravel fractions are river aggregates and therefore show smooth and round shape. Finally, a third generation superplasticizer of the polycarboxylate ether (PCE) type was used to adapt the workability and to adjust the mixes to about the same slump-flow class.

The above described materials have been used to design self-compacting mixes with increasing amounts of PCM. Besides one reference mix without PCM three more mixes were designed containing 1%, 3% and 5% of PCM materials based on their total mass. The applied design method is similar to the SCC mix design of [12]. The method basically focuses on the optimization of the solid granular skeleton. With the help of detailed particle size distributions of all used materials a tailor-graded mix is generated based on an optimized target size distribution including the entire size range of all involved solids. This method has been shown to successfully produce stable SCC mixes as well as other types of concrete like Earth–Moist Concrete with comparable low binder dosages [12,13]. A further benefit of this method is the simple integration of mineral waste materials into concrete mix design. Fig. 2 presents the entire particle size distribution of the reference mix including the target grading and all individual materials, based on the design method elaborated in [13]. The micro-encapsulated PCM material is considered as a particle and therefore part of the optimization. It is not part of the reference mix but for the sake of completeness it is depicted in Fig. 2 as well. The so-called target line follows the grading line of Plum [14], previously referred to as modified Andreasen and Andersen method [12,13]:

$$P(d) = \frac{d^q - d_{\min}^q}{d_{\max}^q - d_{\min}^q} \quad \text{for } q \neq 0 \tag{1}$$

The $d_{\min}$, $d_{\max}$ and q of the target line were 0.224 μm, 16 mm and 0.22, respectively.

3. Estimation of hydration temperature peak for PCM concretes

3.1. Differential scanning calorimetry

A small sample of the micro-capsules has been used for the differential scanning calorimetry (DSC) experiment, deploying a Differential Thermal Analyzer (DTA) Perkin Elmer DSC7. In this research a typical sample mass was around 8 mg for one DSC experiment. A PCM sample was placed in an aluminum pan and sealed with a lid of the same material. The pan containing the sam-

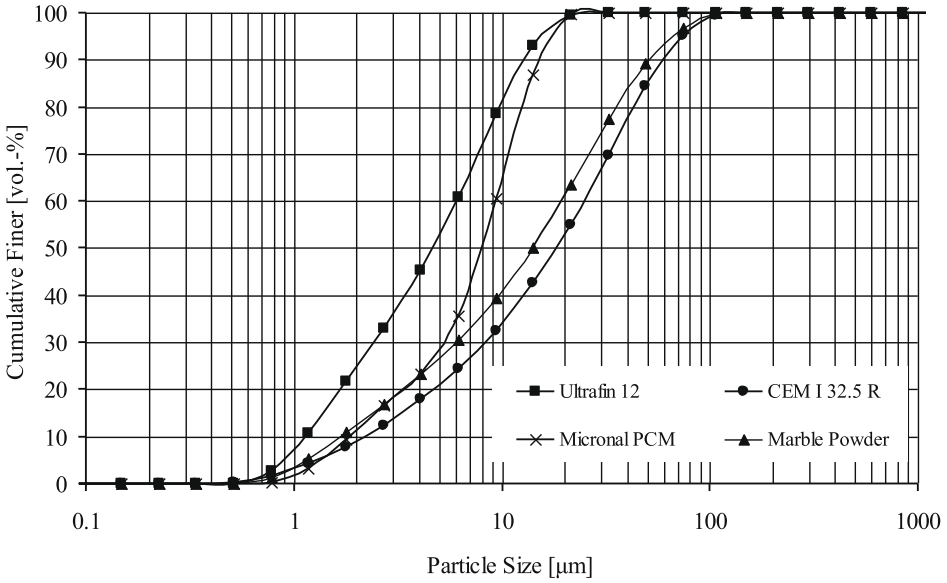

Fig. 1. Particle size distribution of the applied powder types.

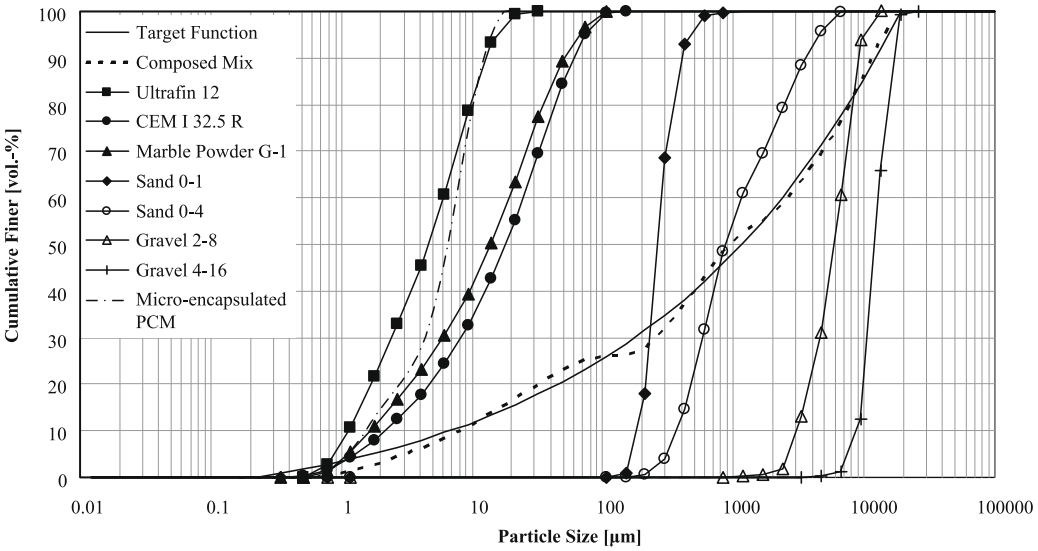

Fig. 2. Plot of the total grading of the PCM reference mix, showing target grading (cp. Eq. (1)) and achieved grading as well as all individual constituents. The PCM capsules are not constituent of the reference mix, but depicted here for the sake of comparison.

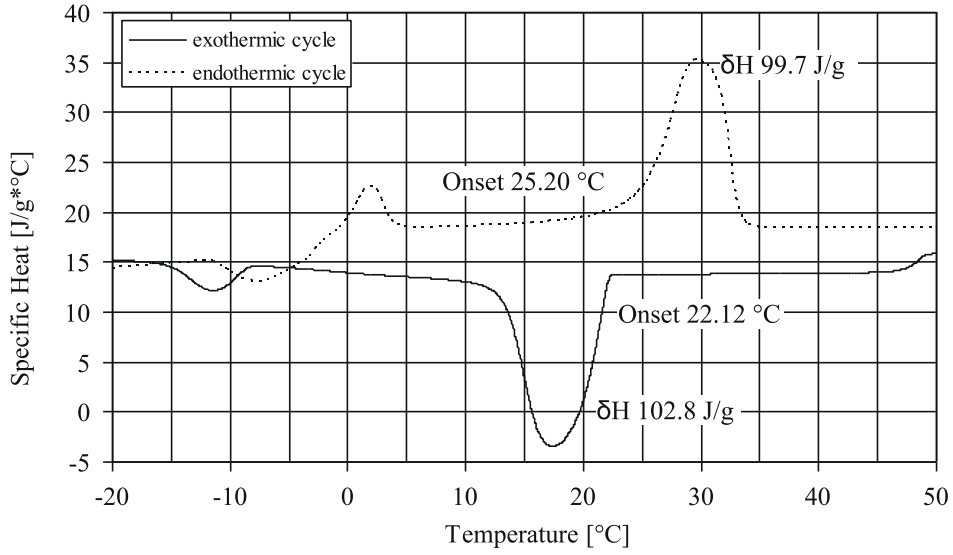

Fig. 3. Plot of specific heat as a function of temperature for the heating and cooling cycles of the applied PCM.

ple as well as an empty reference pan was placed into the furnace of the calorimeter. Afterwards a suitable temperature range for the measurement was selected. This range is in accordance with the expected range of usage and should furthermore comprise the transition temperature of the selected PCM. In the given case a range from −20 °C to 50 °C was selected. For the given temperature range a cyclic heating/cooling/heating scan was conducted at a heating/cooling rate of 10 °C/min with 2 min isothermal holds at both minimum and maximum temperatures. The first cycle started with heating up the sample from −20 °C in order to come to the situation in which all waxes are solidified. For the subsequent cooling and heating cycles solidification and melting enthalpies have been quantitatively estimated by using a linear approximation for the base lines both below and above the melting and solidification peaks. Based on this, during solidification (cooling) an enthalpy δH_{exoth} of 102.8 J/g in a temperature range of 22.1 to 9.3 °C was measured. For the melting (heating) the enthalpy δH_{endoth} amounts to 99.7 J/g in a temperature range of 18.8–35.4 °C. The authors are aware of, that higher values of heating or cooling rate lead to broader melting ranges and vice versa [15]. Fig. 3 provides the heating and cooling scans. The selected heating/cooling rate is responsible for the observed super-cooling effect shown in Fig. 3. This behavior is normally not to be expected when a lower heating/cooling rate of 0.1–0.5 °C/min is applied. Nevertheless, the heating/cooling rate does not influence the total melting/freezing enthalpy. The difference between the solidification and melting enthalpies, shown in Fig. 3, was measured to be 3.1 J/g, which is acceptable according to [16]. A second, smaller peak can be found in a temperature range of about −8 to −16 °C within the cooling cycle. It is assumed that this transition can be assigned to the polymethyl methacrylate shells. For differential calorimetry tests on the hydration of Portland cement the authors would like to refer to [17].

3.2. Concrete temperature modeling during hydration

The following section presents an approach developed for the prediction of the hydration temperature of the deployed specimen

after 1 day curing under semi-adiabatic conditions. These temperatures will be later used for comparison with the results from the semi-adiabatic curing experiment.

The available literature on hydration heat release refers to different models and approaches, like finite element modeling (e.g. [18,19]) or the application of multi-phase hydration models (e.g. [17]). In the following, calculations are provided which allow for the estimation of hydration temperature at a certain age. For the examined case, 1 day was selected given that both deployed cements showed maximum heat release during semi-adiabatic calorimetry tests within the first day. Therefore, in contrast to [3], the ultimate heat of hydration after exactly 1 day was used for the subsequent calculations. The heat release during cement hydration depends on the degree of hydration, which is mainly a function of time and availability of water. Moreover, this model is purely composition depending but does not take into account structural geometry and volume of the test specimen.

According to the second law of thermodynamics the amount of transferred heat, δQ, reads:

$$\delta Q = c_p \cdot m \cdot \delta T \tag{2}$$

where c_p is the specific heat capacity, m is the mass and δT is the temperature difference causing the heat transfer. In the present case δT is the unknown parameter and is caused by the heat release of hydrating cements. Furthermore, the enthalpy of the increasing PCM amount has to be considered for the respective mixes.

In Eq. (2) δQ is the heat energy put into or taken out of the system. This term is in the present case only influenced by the heat produced by the two types of cement (cp. Tables 1 and 2) and the amount of heat consumed (stored) by the melting PCM, as explained in the previous section. Measured heat release values – provided by the cement producers – of the deployed cement types after 1 day of hydration are shown in Table 2. Part of this energy is not consumed for a temperature increase of the concrete, but for the phase transition of the applied PCM. From the differential scanning calorimetry experiment (Fig. 3), it is observed that this enthalpy is equal to $\delta H = 99.7$ kJ/kg. For the calculation of the total specific heat capacity of the concrete mixes the specific heat capacities of the applied materials were taken as: 0.84 kJ/kg K for the cement, 4.19 kJ/kg K for water, 0.74 kJ/kg K for quartzous aggregates and 0.88 kJ/kg K for the marble filler material. The composition of the wax component in the PCM is not specified in detail. However, [20] gives a range of 2.14 to 2.90 kJ/kg K for paraffin wax types. Therefore, 2.40 kJ/kg K was chosen as an average value.

Solving Eq. (2) for δT using the above data in combination with the mix proportions given in Table 1, results in the expected temperature rise in K under totally adiabatic conditions after 1 day of hydration. These temperatures are given in Table 4. Because of the surrounding conditions in which the materials are stored, the temperature of the fresh concrete is expected to be 20 °C.

Table 2
Thermodynamic and strength properties of the deployed materials.

Cement type	Heat release after 1 day $Q_{1\ day}$ (J/g)	Standard strength R_c (N/mm^2)
CEM I 32.5 R	139.3	57.3
Ultrafin 12	250.0	70.0

As can be seen from Table 4, the addition of, for instance, 5% of PCM can theoretically decrease the hydration temperature rise by 24%. Under practical conditions any heat loss to the environment will further decrease the energy source term which finally leads to an even higher apparent efficiency of the PCM material.

4. Experimental procedure

This section addresses the procedure of mixing and the used apparatus for measuring temperature development during hydration.

4.1. Concrete mixing

The mixing of the self-compacting PCM mixes took place in four steps. At first all solids except for the PCM are mixed for 30 s in order to homogenize the dry components. Thereafter, about 90% of the total water dosage is added and mixing is continued for further 2 minutes. In this range of time the superplasticizer is added directly after the water in order to assure sufficient mixing time for the plasticizer to be homogeneously dispersed and activated. At this latest possible moment the micro-encapsulated PCM is added to the mixing process in order to expose it as short as possible to the mixing process. After the PCM addition, part of the remaining SP and water is dosed to, again, obtain the desired self-compacting characteristics. This is for the time being controlled by visual inspection. A subsequent slump-flow and V-funnel test decides if an additional water or SP dosage is necessary to obtain equal workability in terms of relative viscosity and yield stress. All four mixes succeeded in achieving similar workability with only one additional dosage step. Table 1 refers to the final water and SP dosages used for the respective mixes.

4.2. Semi-adiabatic curing

To measure the influence of PCM content on the peak temperature during hydration, an experimental setup has been constructed. A layer of cellular glass, 160 mm thick with a heat resistance of 3.81 m^{2}K/W, forms a semi-adiabatic environment for four standard cubic molds with an edge length of 150 mm according to EN 12390-1. The box-shaped environment measures

Table 1
Mix composition (total volume: 1000 dm^3).

	Reference mix		1% mix		3% mix		5% mix	
	Volume (dm^3)	Mass (kg)	Volume (dm^3)	Mass (kg)	Volume (dm^3)	Mass (kg)	Volume (dm^3)	Mass (kg)
Ultrafin 12	47.6	149.9	47.6	149.9	47.6	149.9	47.6	149.9
CEM I 32.5 R	95.5	299.7	95.5	299.7	95.5	299.7	95.5	299.7
Marble powder	60.8	170.2	35.8	98.0	0.0	0.0	0.0	0.0
PCM	0.0	0.0	24.9	23.3	76.6	70.0	124.3	113.7
Sand 0–1	53.0	139.6	53.0	139.6	53.0	139.6	53.0	139.6
Sand 0–4	248.1	655.3	248.1	655.3	248.1	655.3	248.1	655.3
Gravel 2–8	147.7	387.1	147.7	387.1	147.7	387.1	147.7	387.1
Gravel 4–16	122.7	319.6	122.7	319.6	122.7	319.6	122.7	319.6
SP glenium 51	2.9	3.1	2.9	3.1	2.3	2.4	2.8	2.9
Water	203.2	203.2	207.4	207.4	211.5	211.5	248.4	248.4
Air	13.0	–	13.0	–	13.0	–	13.0	–

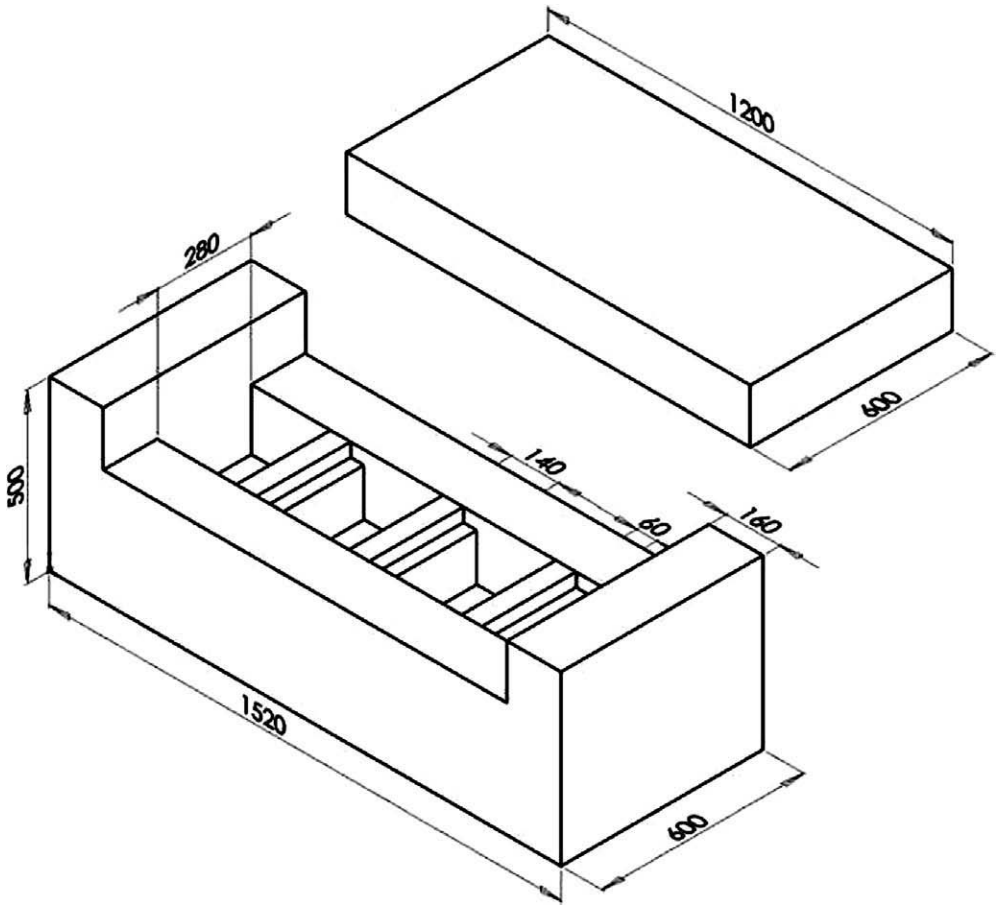

Fig. 4. Depiction of the semi-adiabatic environment for four standard sized molds.

1520 mm × 600 mm × 500 mm ($l \times w \times h$). The four molds were individually separated by three fixed septa of 50 mm cellular glass (see Fig. 4). Around and within the molds thermocouples (type *T*) were placed to measures the temperature during the early stage of hydration. Data acquisition took place by using National Instruments USB-6215 and PICOs TC-08 in combination with a personal computer to store the data. The basis of this setup is comparable to setups used before [21,22].

4.3. Thermal conductivity measurements

A "CT-METRE" was used for the conductivity measurements. The device uses the transient hot wire method conforming to ISO 8894-1:1987, DIN 51046 and ASTM D2326. The operating principle is based on the association of a heating device with a temperature sensor (both connected inside the same probe) intended to measure the temperature increase undergone by the sensor during a predetermined heating time. The method is not applicable when a phase change occurs in the material, as might be the case with the PCM containing mixes. To overcome the problem, the samples have been heated to 30 °C and the measurements have been performed at this temperature, which is well above the melting range of the PCM.

4.4. Specific heat capacity/thermal efficiency measurements

Unlike thermal conductivity, specific heat capacity (c_p) increases rapidly in the temperature range of phase change. This makes transient methods inappropriate for c_p measurements. The Differential Scanning Calorimetry method requires a representative sample of the material in the order of a few milligrams which is not possible with concrete samples consisting of particles up to 16 mm diameter. For the needs of inexpensive and reliable measurements an experimental setup (Fig. 5) has been developed which allows measurements of heat capacity, thermal mass and thermal efficiency of building materials. The device applies variable thermal loads at the two sides of a flat-surface material sample, while measuring its thermal response. An extensive

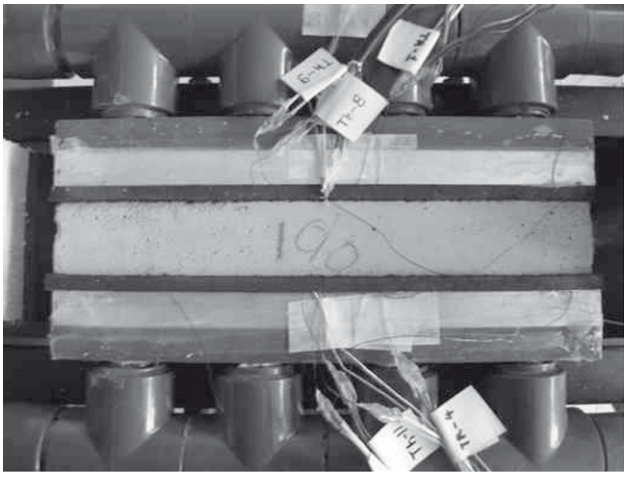

Fig. 5. Sample holder of the thermal mass measuring device (sample placed between two thermo-regulated plates).

presentation of the concept and the corresponding operational principle can be found in [23].

5. Results

5.1. Effects on the properties of fresh concrete

In order not to expose the PCM micro-capsules to additional wear during pouring and compaction, a self-compacting mix was designed. These mixes start flowing at much lower yield stresses compared to plain concrete. Therefore, the concrete placing involves only a limited amount of shear stress for the micro-capsules. Another reason for the choice of SCC is the faster heat development of SCC compared to standard plain concrete which is among others reported by Ye et al. [24].

For the reader interested in SCC, in the following a brief summary on the most important SCC related properties is given. These measures have been determined in order to show that the workability was kept similar for all mixes by a respective adjustment of water and plasticizer content. Variations in the hardened concrete properties can, hence, not result from different levels of workability but be assigned to the varying amounts of PCM. For the assessment of self-compacting abilities three standard tests were conducted. These are the V-funnel test as a measure for the relative viscosity, the slump-flow test to assess the yield stress and fluidity, and the J-ring test which shows the blocking behavior of fresh mixes. In Table 3 these measures are summarized for all mixes including the reference mix not containing PCM.

In general, from the data presented in Table 3, it can be concluded that all four mixes show similar good self-compacting properties. The 3% and 5% mixes exhibit slightly higher viscosity which mainly is caused by the water dosage. In case of the other measures all mixes show a similar range. The stability time, which is notably below one second for all mixes, identifies stable SCCs. Furthermore, the tendency to blockage can be assessed, judged on the J-ring step, to be small. An analysis of the slump-flow measures results in a very narrow range of flow diameters (740–770 mm). This implies that, according to the EFNARC SCC guidelines [25], these mixes can be classified into two slump-flow classes (SF2 and SF3) since 750 mm is the separation criterion of both classes. The required SP dosage was only 2.4–3.1 kg per cubic meter concrete. Furthermore, no other auxiliary admixtures, such as viscosity modifying agents, were needed.

In summary all four mixtures resulted in good and partly excellent self-compacting properties. The increasing PCM dosage did not seem to influence any of these measures in a verifiable range. Only the visual inspection during the V-funnel and in particular the slump-flow experiments resulted in some uncommon observations. Here a white liquid was accumulated on top of the mixture in areas of slow flow or on resting concrete areas. This observation

Table 3
Fresh concrete properties regarding the self-compactibility.

Fresh concrete property	Reference mix	1% mix	3% mix	5% mix
V-funnel time (s)	3.2	3.7	10.5	6.6
V-funnel time 5 min (s)	3.2	4.0	11.2	7.2
Stability time (s)	0	0.3	0.7	0.6
Slump flow (mm)[a]	760	745	770	740
Slump flow with J-ring (mm)[a]	680	720	770	760
J-ring step (mm)	9.75	10	5.5	4.75
t_{50}-time (s)[a]	2.4	1.4	3.6	2.4
Fresh concrete temperature (°C)	22.5	23.0	22.5	22.5

[a] The inverted cone method was applied.

Fig. 6. SCC after J-ring test with obvious white flow marks behind the rods (in flow direction) and around the spreading concrete.

became especially obvious at the flow area behind the rods of the J-ring as well as along the circumferential line of the spreading concrete during slump-flow tests (cp. Fig. 6). This behavior was only observed for the three mixes containing PCM and also became more prominent with increasing PCM content.

5.2. Effects on the hydration temperature peak

The setup offers space to store four molds in an environment of 20 ± 2 °C. After casting, the temperature development of the four kernels was monitored for 5000 min, taking measurements every minute. These results are shown in Fig. 7.

The reference mix shows a peak temperature of 41 °C. This temperature is significantly lower than the results of [21] have shown for other Portland cement mixtures during hydration. The observed cooling refers to a leakage of heat which is a proof of the semi-adiabatic characteristics of the setup. Otherwise, under totally adiabatic conditions, a temperature rise of about 76 °C to an absolute temperature of 98 °C would be expected, considering complete hydration of the cement. For very massive constructions, where adiabatic conditions can be assumed for the core volume, such a temperature rise would imply the boiling of the free water and cause fundamental durability problems.

Fig. 7 shows that an increasing amount of PCMs results in a lower peak temperature. Because of the comparable availability of internal or chemical energy in all four mixes, more time is needed to come to the ambient temperature when the amount of PCMs is higher. The 3% and 5% PCM mixes show a small bow around 25 °C, being – according to the DSC experiment – the onset for the endothermic cycle.

The modeling of maximum hydration temperatures for PCM concretes resulted in temperatures of 44.1 °C for a mix containing 5% PCM to 51.7 °C for a mix containing 1% PCM, starting with a temperature of 20 °C for the fresh concrete (see Table 4). During the experiments the starting temperatures were 2.5–3.0 °C higher, but the peak temperatures were lower. The differences between the four mixes are shown in Table 4. Surprisingly, the 3% mix had a larger temperature rise than the 1% mix. In this case it could be that (1) the adiabatic surrounding did not suffice, that (2) more PCM particles were destroyed during mixing in the 3% mix than in the 1% mix, or that (3) the thermocouples were not able to register the temperature correctly. In future experiments these three aspects will be taken in consideration.

Regarding option number two, the analysis of the porosity using SEM showed that many PCM capsules were in fact destroyed. Nevertheless, the temperature registration showed that to a large extent, especially in the 5% mix, the peak temperature could be

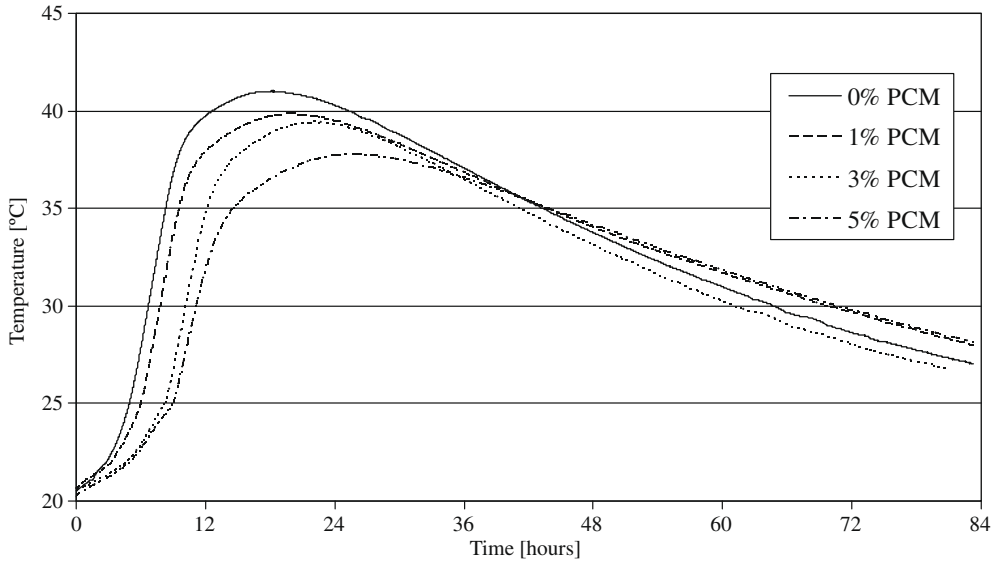

Fig. 7. Temperature development of four self-compacting mixes in the kernel of the molds in a semi-adiabatic environment during the first 3.5 days after casting.

Table 4
Temperature rise for the given mixes according to computations and experiments.

Mix	Reference mix	1% mix	3% mix	5% mix
Temperature rise by model (K)	31.7	30.7	28.3	24.1
Absolute temperature by model (°C)	54.2	53.7	50.8	46.6
Decrease compared to reference mix (%)	–	3.1	10.6	23.8
Temperature rise in experiment (K)	18.5	16.8	16.9	23.7
Absolute temperature in experiment (°C)	41.0	39.8	39.4	37.6
Decrease compared to reference mix (%)	–	9.2	8.6	28.1

lowered. This could imply that, despite the partial destruction of the PCM capsules, a large part of the wax is still present in the concrete and could be potentially functioning. This hypothesis is subject of ongoing tests. Although the wax seems to be able to store latent heat, new mix procedures and more resilient shells (mechanical/chemical) should be developed to lower the amount of damaged micro-encapsulated particles (cp. [27]).

5.3. Effects on mechanical properties

The effects of PCM on the mechanical properties of concrete are discussed by addressing compressive strength, intrinsic density and porosity.

5.3.1. Compressive strength

In order to evaluate the effect of PCMs on the mechanical properties of concrete, compressive strength measurements were executed. Therefore, five standard cubes per mixture with an edge length of 150 mm according to EN 12390-1 (2000) have been tested at the 28th day after production. The test procedure for compressive strength is conforming to EN 12390-3 (2001).

Since a new mix design, as described in Section 2, has been applied to this concrete, elevated strength compared to standard composition with equal cement content was expected. Therefore, a modification of Féret's equation was applied to get an indication for the possible compressive strength at 28 days [26]. This modification includes the contribution of other cementitious materials and reads as:

$$f_c = \frac{K_g R}{\left(1 + 3.1 \frac{W+A}{C(1+K_1+K_2)+BFS}\right)} \quad (3)$$

where k_g is an aggregate coefficient (typical values are 5.4 for crushed aggregates and 4.8 for rounded aggregate), R_c is the standard cement strength (cp. Table 2), W is the total effective water content, A is the volume of entrapped air and C is the weight of cement (in kg/m^3). The other variables, K_1, K_2 and BFS, refer to pozzolanic and latent hydraulic effects. Since none of these materials were used, these latter variables are zero. Including the relevant data in Eq. (3), the expected strength of the reference mix can be calculated to 46.2 N/mm^2. In fact a compressive strength of 74.1 N/mm^2 was determined. The significantly higher strength could for a large extent be attributed to the improved packing of the new mix design.

Results of the compressive strength measurement are presented in Fig. 8. From the given data it can be clearly observed that increasing PCM dosages lead to significantly lower compressive strengths.

From Fig. 8 it can furthermore be concluded that the compressive strength of this specific mixture decreases by 13% for each additional percentage of PCM. This linear relation holds for the range of PCM contents considered.

5.3.2. Porosity and intrinsic density

An analysis by means of scanning electron microscopy shows a porous micro-structure and many, spherical voids which presumably contained PCM capsules before. As a mixture of paraffin

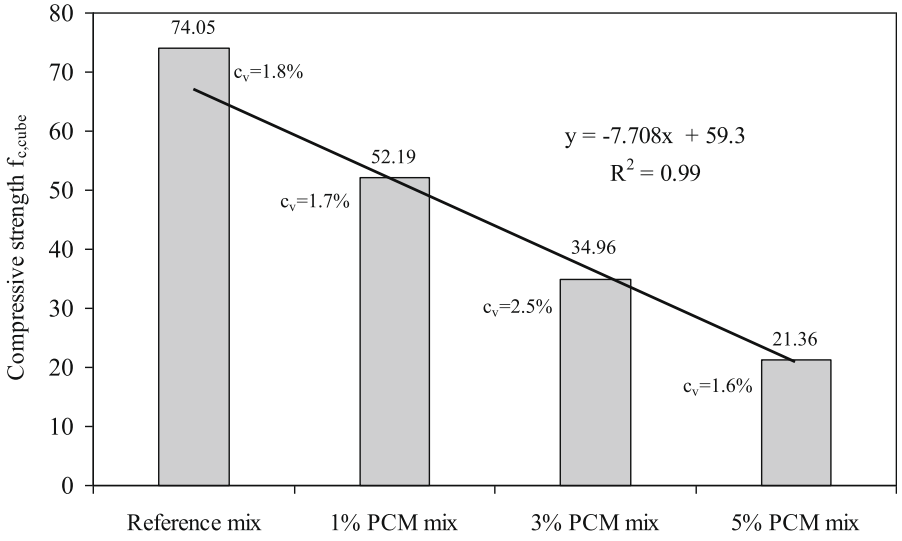

Fig. 8. Compressive strength of the PCM mixes after 28 days (N/mm^2) including the coefficient of variation (c_v) of each mix.

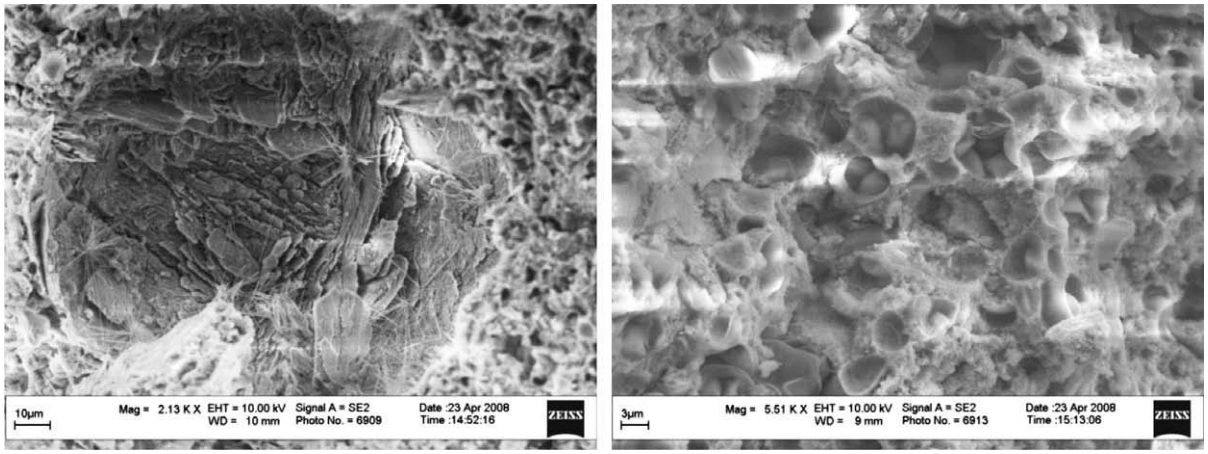

Fig. 9. SEM micrographs of (left) an open pore covered with solidified wax, and (right) a higher magnified (5.5 k) part of the matrix with deformed and broken capsules, partly pure leaked wax is visible.

probably also slightly varies in its melting temperature, softer paraffin melts earlier than the harder paraffin components. This causes a slight segregation during the melting process. Due to the immiscibility of the leaked paraffin with other concrete ingredients, solidification appears in the cavity of the matrix and at pore walls. An example is given with the SEM micrograph in Fig. 9 (left). Here flaked structures of solidified wax cover the inner walls of the pore. Close to the pore walls it forms a type of cell wall which appears to be smooth from the outside (cp. left boundary). The surrounding structure is densely occupied with PCM capsules of the predominant size of about 6 µm (cp. Fig. 9 right). These capsules appear to a large extent deformed and broken. These observations are very similar to those by Gschwander et al. [27], who found broken micro-capsules of the same type after pumping PCM slurries. For the SEM analysis a Zeiss 1550 HR SEM was applied. The samples have been scanned in uncoated state with low acceleration voltage.

The presence of the broken and deformed capsules has been studied in a side experiment. Hereby the respective encapsulated PCM was mixed with a supersaturated water-fine sand suspension (pH 7) in a standard planetary mortar mixer. Already after short mixing time (3 min) pure paraffin leaked from the broken capsules and floated on the water surface. This can be doubtlessly proven by an olfactory test and visual observation. It can be assumed that intensive mixing in a horizontal concrete mixer produces more shear stress, which will have a negative effect on the encapsulated wax. Furthermore, to prove the chemical resilience, especially the pH influence, aqueous sodium hydroxide (NaOH) solutions with different pH value have been produced. The respective micro-encapsulated PCM was added to these solutions without applying any mixing energy. Also in this case already after a short time wax was floating on top of the solution having pH values equal to 7 and higher.

In addition to strength measurements the development of intrinsic density (ρ_{int}) has been carried out for increasing PCM quantities. The density measurement was executed according to EN 12390-7 (2000). Deviating from this standard the total water absorption was started after evacuating the air from the specimens using a vacuum desiccator. Based on the values of the density a measure for the open porosity was calculated. This value represents the part of the void fraction which is open to the surface and therefore can be penetrated during the underwater storage. The open porosity [%, v/v], *oP*, reads as:

$$oP = WA\frac{\rho_{int}}{\rho_{water}} \tag{4}$$

with *WA* being the water absorption [%, m/m]. The water absorption is the ratio of the mass difference between saturated and dried specimen to the mass of the oven dry specimen. Values for intrinsic density and porosity are presented in Fig. 10.

Fig. 10 shows that the concrete density is decreasing with growing PCM content. This can firstly be explained by the low density of the PCM (0.915 g/cm^3) and secondly by a structural change of concrete packing density, which is revealed by its increasing porosity.

5.4. Effects on the thermal properties of hardened concrete

The study of the effects of PCM on the thermal properties of concrete includes measurements of thermal conductivity and specific heat capacity.

5.4.1. Thermal conductivity

In order to evaluate the effect of PCM on the thermal conductivity of concrete three mixes containing 1% PCM, 3% PCM and 5% PCM per weight, and a reference material were measured.

According to the standards, two samples of 100 mm × 100 mm × 50 mm of every mixture were prepared for the measurements. Thermal conductivity measurements are presented in Fig. 11. It is clearly indicated that the addition of PCM particles into the mass of the concrete results in a reduction of thermal conductivity. This can be explained by the enhanced air content and by the lower thermal conductivity of paraffin.

5.4.2. Specific heat capacity/thermal mass

For the specific heat capacity measurements four samples of the four different mixes were prepared at the appropriate dimensions, 200 mm × 200 mm × 30 mm ($l \times w \times h$). The samples were introduced in the sample holder of the thermal analysis device at a temperature of 19 °C and were heated up to 28 °C. The temperature of the device during the heating process was maintained constant at 32 °C. The temperature of the samples and the heat flux from the device to the samples were recorded. Temperature and heat flux measurements allow the calculation of the heat capacity and thermal mass of the samples (Figs. 12 and 13) as:

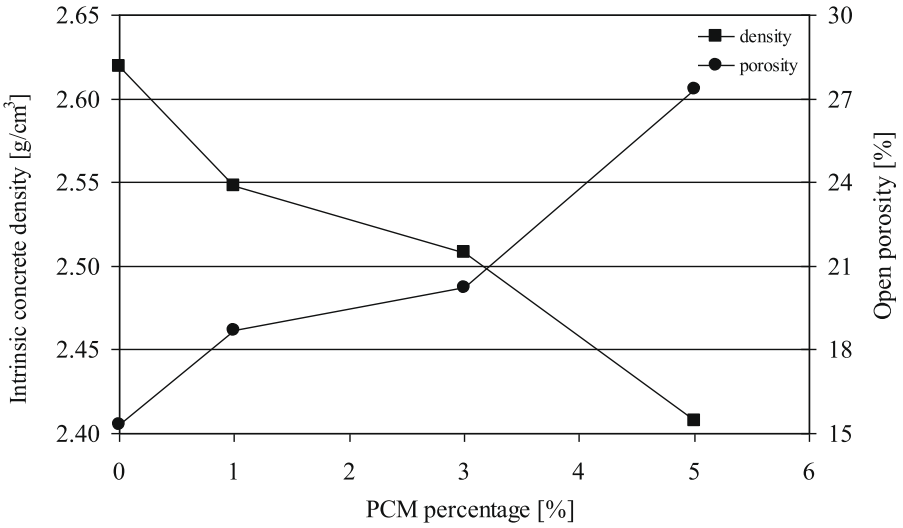

Fig. 10. Plot of density and open porosity versus the PCM dosage in % (m/m).

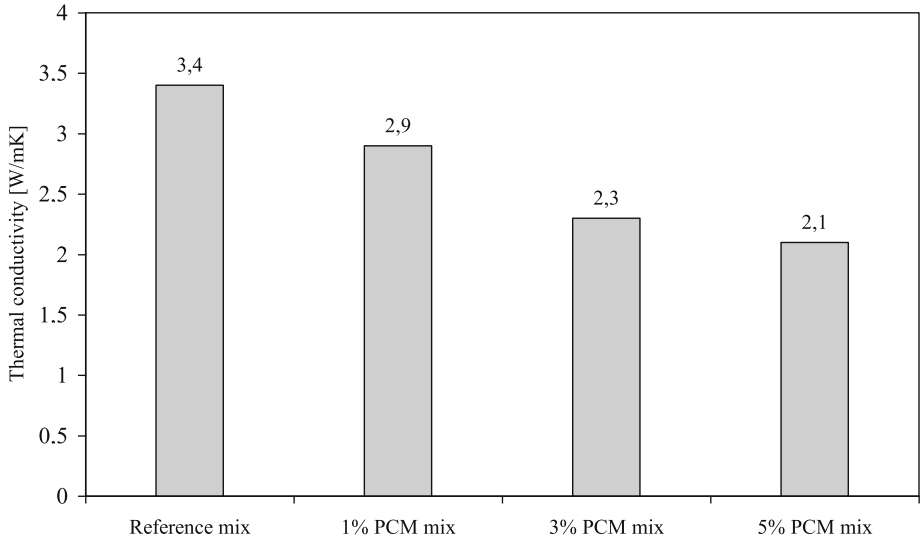

Fig. 11. Thermal conductivity of the PCM mixes.

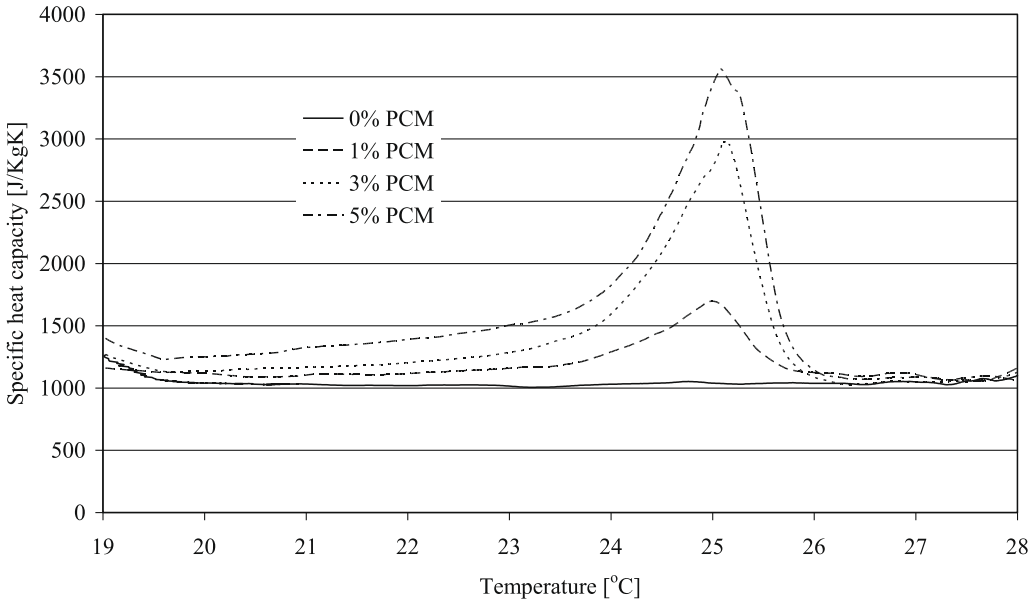

Fig. 12. Specific heat capacity of the PCM mixes versus temperature.

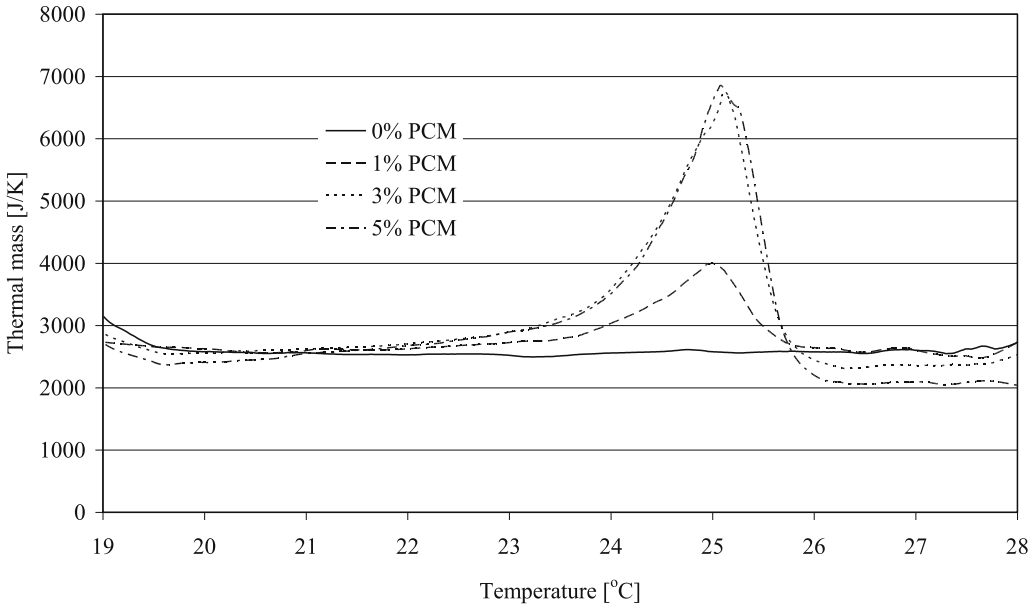

Fig. 13. Thermal mass of the PCM mixes versus temperature.

$$c_p = \frac{A\dot{q}}{m(\frac{dT}{dt})} \quad (5)$$

$$M_{\text{th}} = mc_p \quad (6)$$

where c_p is the heat capacity of the sample, M_{th} the thermal mass, A the heat exchange area of the sample, $\dot{q}$ the heat flux per square meter, m the mass of the sample, T the temperature of the sample and t the time.

Figs. 12 and 13 present the measured specific heat capacity and thermal mass for the four samples versus temperature. In both Figures, the effect of increasing the percentage of PCM in the mixture is apparent in the melting temperature range of the PCM (23–26 °C). Comparison of Figs. 12 and 13 indicates that, as expected, increasing the amount of PCM in the mixture increases significantly its specific heat capacity (up to 3.5 times for the 5% PCM content). However, there seems to be an upper limit to the increase of the thermal mass. The 5% PCM mixture has slightly more thermal mass than the 3% mixture inside the melting range of the PCM but less outside of this region. This can be the consequence of decreasing concrete density with increasing PCM content. As a result, a percentage more than ca. 5% (or 4%) of PCM in the mixture does not increase the thermal mass of the material.

5.5. Effect of PCM quantity on thermal performance

Evaluation of thermal performance of building materials used for building envelopes is generally performed by measuring the decrement factor and time lag. In the case of building materials containing PCM, the above two measures may not be representative since they do not take into account the large amount of heat contributions/subtractions in the temperature range that the phase change occurs [28]. An appropriate method of evaluating the effect

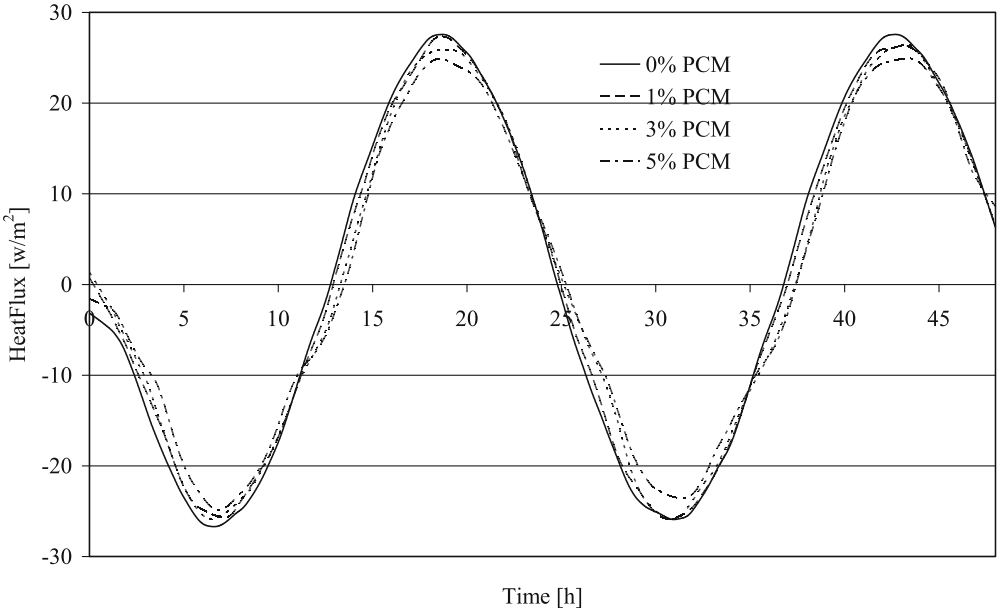

Fig. 14. Heat flux on the side of the sample corresponding to the indoor wall surface.

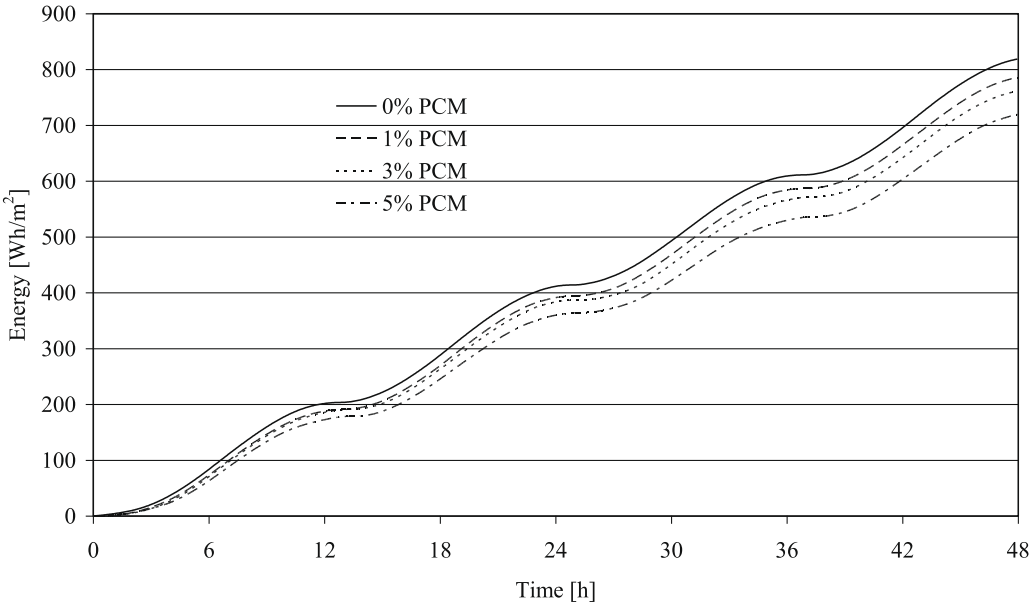

Fig. 15. Energy required for maintaining indoor temperature stable at 23.5 °C.

of PCM on thermal efficiency of structural elements is the comparison of the heat flux at the indoor surface of a wall with different amounts of PCM [29].

In the current work the above described thermal analysis device is used to simulate indoor and outdoor temperatures and the corresponding temperature profiles are imposed at the two sides of the sample. The outdoor temperature is assumed to have a sinusoidal variation from 18.5 °C to 28.5 °C for 48 h (for instance resembling temperature variations in a South European country), while the indoor temperature is set stable at a level of 23.5 °C. Temperatures and heat fluxes on both surfaces of the same samples as the ones used for the specific heat capacity measurements are recorded.

Integration of the measured heat flux (Fig. 14) on the inner side of the sample provides a measure of the total heat losses towards the indoor environment (Fig. 15). The heat flux measurements of Fig. 14 demonstrate an up to 11% variation in the measured maximum and minimum peak values for the sample with 5% PCM content. The calculated energy (Fig. 15) corresponds to the energy required by an air-conditioning system to maintain the indoor temperature constant at 23.5 °C. Savings up to 12% can be expected as a result of the inclusion of 5% PCM in the mix.

The measured total "energy consumption" under the above conditions in 48 h for the 0%, 1%, 3% and 5% mixtures is shown in Table 5. As can be seen, PCM mixes improve significantly thermal performance of concrete in terms of energy saving. This is not only due to the increased thermal mass (the 3% and 5% mixes have similar thermal masses) but also due to the improvement in thermal insulation (conductivity reduction).

Table 5
Total energy consumption and decrease compared to reference mix.

Mix	Reference mix	1% mix	3% mix	5% mix
Total energy consumption in 48 h (Wh/m^2)	819	786	761	720
Decrease compared to reference mix (%)	–	4	7	12

6. Conclusion

The mix design method presented in [12] for SCC containing marble powder was successfully adopted and applied to the three mixes containing micro-encapsulated PCM. Based on the J-ring and V-tunnel test, all four mixtures featured good self-compacting properties. Using the developed recipes the increasing PCM dosage did not seem to influence the properties of the fresh concrete.

The modeling and experiments involving hydration showed that the temperature peak of hydration could be reduced up to 28.1% by increasing the PCM content to 5%. However, the heating rate cannot be changed by the PCM, only the absolute temperature peak is lowered by the amount of energy temporarily stored in the PCM. The emission of heat from the sample will therefore continue for a longer time when the PCM content is higher. A similar behavior can be observed by adding ice to the mixing process, which is a common technique for concreting in hot climates. The inclusion of ice as part of the mixing water is highly effective for the reduction of hydration temperature because of the latent heat (335 kJ/kg) taken from the melting ice [30].

Regarding the thermal properties of hardened self-compacting concrete with PCM, the experiments showed a reduction of thermal conductivity with increasing amounts of PCM.

The measurements have indicated that the overall behavior of each sample is the combined result of conductivity and specific heat variations. The porosity of the samples is increased – with consequent density decrease – with increasing PCM content. The increased porosity would be expected to lead to lower thermal mass values, but the presence of the PCM results in totally opposite behavior in the phase change region. Namely, with increasing PCM content the thermal mass of the sample increases significantly. Although the specific heat capacity increased with increasing amount of PCM in the considered temperature range (24–26 °C), the thermal mass seems to be bound by a maximum of approximately 6800 J/K at 4–5% PCM.

The increase in thermal mass could improve significantly the thermal performance of concrete in terms of energy saving. For example, savings up to 12% could be expected as a result of the inclusion of 5% PCM in the mix.

More experiments with samples incorporating dedicated amounts of PCM around these percentages could provide better insight into the exact value of this maximum. In practice, both the lower thermal conductivity and the increased heat capacity significantly improve the thermal performance of concrete and could lead to energy savings in building applications.

Although the loss of compressive strength is significant, concrete with PCM content up to 3% and an accompanying compressive strength of 35 N/mm^2 is still for most constructional purposes very well acceptable. The loss of compressive strength can be assigned to destructed shells of the PCM capsules for reasons mentioned in Section 5.3.2. Both observations made during that side experiment show that the respective micro-encapsulated PCM material is not suitable for the requirements of a concrete application. The released wax from the micro-capsules interferes into the surrounding concrete matrix and hinders a sufficient strength development in multiple ways. Here, the possible inhibition of the water transport and hence an interruption of the hydration, and the possible development of phase interfaces by the wax are to be mentioned. Therefore, the main recommendation to be given involves the development of stronger shells for micro-encapsulated PCM. These stronger shells have to withstand the highly alkaline conditions, which in addition to the mechanical impact have a negative influence on the strength of the shells.

Acknowledgements

The authors wish to express their sincere thanks to SenterNovem and the European Commission (I-Stone Project, Project No. 515762-2) and the following sponsors of the UT research group: Bouwdienst Rijkswaterstaat, Rokramix, Betoncentrale Twenthe, Graniet-Import Benelux, Kijlstra Beton, Struyk Verwo Groep, Hülskens, Insulinde, Dusseldorp Groep, Eerland Recycling, Enci, Provincie Overijssel, Rijkswaterstaat Directie Zeeland, A&G Maasvlakte, BTE, Alvon Bouwsystemen, V.d. Bosch Beton (chronological order of joining). Furthermore, their gratitude goes to BASF and Foamglas for providing materials.

References

[1] Pérez-Lombard L, Ortiz J, Pout C. A review on buildings energy consumption information. Energy Build 2008;40:394–8.
[2] Khudhair AM, Farid MM. A review on energy conservation in building applications with thermal storage by latent heat using phase change materials. Energy Convers Manage 2008;45:263–75.
[3] Bentz D, Turpin R. Potential applications of phase change materials in concrete technology. Cem Concr Compos 2007;29(7):527–32.
[4] Mondal S. Phase change materials for smart textiles – an overview. Appl Therm Eng 2008;28:1536–50.
[5] Ismail KAR, Henrìques JR. PCM glazing systems. Int J Energy Res 1997;21:1241–55.
[6] Ismail KAR, Castro JNC. PCM thermal insulation in buildings. Int J Energy Res 1997;21:1281–96.
[7] Tyagi VV, Buddhi D. PCM thermal storage in buildings: a state of art. Renew Sust Energy Rev 2007;11:1146–66.
[8] Kuznik F, Virgone J, Noel J. Optimization of a phase change material wallboard for building use. Appl Therm Eng 2008;28:1291–8.
[9] Pasupathy A, Velraj R, Seeniray RV. Phase change material-based building architecture for thermal management in residential and commercial establishments. Renew Sust Energy Rev 2008;12:39–64.
[10] Sharma A, Tyagi VV, Chen CR, Buddhi D. Review on thermal energy storage with phase change materials and applications. Renew Sust Energy Rev 2009;13(2):318–45.
[11] Taylor HFW. Cement chemistry. 2nd ed. London: Thomas Telford Publishing; 1997.
[12] Hunger M, Brouwers HJH. Natural Stone waste powders applied to SCC mix design. Restor Build Monuments 2008;14(2):131–40.
[13] Hüsken G, Brouwers HJH. A new mix design concept for earth–moist concrete: a theoretical and experimental study. Cem Concr Res 2008;38:1246–59;
Hüsken G, Brouwers HJH. A new mix design concept for earth–moist concrete: a theoretical and experimental study. Cem Concr Res 2009;39:832.
[14] Plum NM. The predetermination of water requirement and optimum grading of concrete: under various conditions. Studie Nr. 3. Copenhagen. The Danish National Institute of Building Research – Statens Byggeforskningsinstitut: 96; 1950.
[15] Mehling H, Ebert HP, Schossig P. Development of standards for materials testing and quality control of PCM. In: Proceedings of 7th conference on phase-change-materials and slurries. Dinan, Frankreich; 2006.
[16] Bentz D. A computer model to predict the surface temperature and time-of-wetness of concrete pavements and bridge decks. US Department of Commerce, NISTIR 6551; 2000.
[17] Meinhard K, Lackner R. Multi-phase hydration model for prediction of hydration-heat release of blended cements. Cem Concr Res 2008;38:794–802.
[18] Buffo-Lacarriere L, Sellier A, Escadeillas G, Turatsinze A. Multiphasic finite element modeling of concrete hydration. Cem Concr Res 2007;37(2):131–8.
[19] Verma P, Varun, Singal SK. Review of mathematical modeling on latent heat thermal energy storage systems using phase-change material. Renew Sust Energy Rev 2008;12:999–1031.
[20] Diracdelta. Specific heat capacity. Diracdelta.co.uk Science and Engineering Encyclopedia, Dirac Delta Consultants Ltd., Warwick, England; 2008 [retrieved 18.06.08].
[21] Liwu M, Min D. Thermal behavior of cement matrix with high-volume mineral admixtures at early hydration age. Cem Concr Res 2006;36:1992–8.

[22] Jones MR, McCarthy A. Heat of hydration in foamed concrete: effect of mix constituents and plastic density. Cem Concr Res 2006;36:1032–41.
[23] Mandilaras I, Founti M. Experimental investigation of agglomerate marbles containing phase change materials. In: 11th international conference on thermal energy storage-EffStock, Stockholm, Sweden; 2009.
[24] Ye G, Liu X, De Schutter G, Poppe AM, Taerwe L. Influence of limestone powder used as filler in SCC on hydration and microstructure of cement pastes. Cem Concr Compos 2007;29(2):94–102.
[25] EFNARC – The European Federation of Specialist Construction Chemicals and Concrete Systems. The European guidelines for self compacting concrete – specification, production and use; 2005.
[26] Hu C, Saucier F, Lanctôt MC, Clavaud B. Investigation on the strength limit of very high strength concretes. In: 5th international symposium on utilization of high strength/high performance concrete. Sandefjord, Norway; 1999.
[27] Gschwander S, Schossig P, Henning HM. Micro-encapsulated paraffin in phase-change slurries. Sol Energy Mater Sol Cells 2005;89(2–3):307–15.
[28] Zhang Y, Lin K, Jiang Y, Zhou G. Thermal storage and nonlinear heat-transfer characteristics of PCM wallboard. Energy Build 2008;40:1771–9.
[29] Alawadhi EM. Thermal analysis of a brick containing phase change material. Energy Build 2008;40:351–7.
[30] Kay EA. Hot and cold weather concreting. Adv Concr Technol Set 2003:1–18.